

# Spinon confinement in a spin-1 chain

Laurens Vanderstraeten,<sup>1</sup> Elisabeth Wybo,<sup>1,2</sup> Natalia Chepiga,<sup>3</sup> Frank Verstraete,<sup>1</sup> and Frédéric Mila<sup>4</sup>

<sup>1</sup>*Department of Physics and Astronomy, University of Ghent, Krijgslaan 281, 9000 Gent, Belgium*

<sup>2</sup>*Department of Physics and Institute for Advanced Study,  
Technical University of Munich, 85748 Garching, Germany*

<sup>3</sup>*Institute for Theoretical Physics, University of Amsterdam,  
Science Park 904, 1098 XH Amsterdam, The Netherlands*

<sup>4</sup>*Institute of Physics, Ecole Polytechnique Fédérale de Lausanne (EPFL), CH-1015, Lausanne, Switzerland*

We explain how spinons and magnons naturally arise in  $SU(2)$  invariant spin chains when describing ground states and elementary excitations using MPS. Within this description, spinons can emerge in a spin-1 chain at a first-order transition between a symmetry-protected topological phase and a trivial phase. We provide MPS simulations for the spinon dispersion relations in a frustrated and dimerized spin-1 chain, and show that these spinons determine the low-lying spectrum in the vicinity of this transition by the formation of spinon/anti-spinon bound states.

In 1982, Faddeev and Takhtajan published a paper with the enigmatic title “What is the spin of a spin wave?” [1, 2]. In this paper, the authors showed that the elementary excitation in the spin-1/2 Heisenberg antiferromagnetic chain is a spin-1/2 doublet, contrary to the received picture that the spectrum consists of a triplet of spin-1 waves [3]. They consider these excitations to be particles—later, they were called spinons [4, 5]—by virtue of their localized nature and the fact that one can consider their scattering. All physical states, i.e. the states that can be created by acting with a local operator on the ground state, consist of an even number of these spinon states. Around the same time, Shastry and Sutherland proposed the spin-1/2 soliton to be the elementary excitation in dimerized spin-1/2 chains [6], similar to the solitons in dimerized long-chain polymers [7]. Again, the solitons are considered to be localized spin-1/2 particles and only two-particle states connect to the ground state through a local operator.

Later on it was realized that adding extra terms in the spin-chain hamiltonian can lead to the confinement of these fractionalized particles. For example, adding an explicit dimerization to the dimerized spin chain leads to an effective linear potential between the solitons and, therefore, to their confinement [8–10]. With the spinons no longer existing as well-defined particles, the spectrum of such an extended model consists of a stack of spinon/anti-spinon bound states [11]. The phenomenon of spinon or soliton confinement has non-trivial effects in the real-time dynamics of spin chains as well [12, 13].

Spinons in quantum spin chains were among the first instances of collective excitations with fractional quantum numbers, and are at the basis of many exciting developments in strongly-correlated quantum physics. In particular, it was gradually realized that fractionalized excitations are typically supported by a ground state that exhibits some form of topological order. This connection between topological order and fractionalized excitations can be naturally understood within the language of tensor networks. In this language, a quantum ground state is represented as the contraction of an extensive number of local tensors, where the topological properties of the

global state are encoded as symmetries of the local tensors [14]. Fractionalized excitations are represented as either defects in the symmetry pattern of the ground-state tensors [15, 16] or local perturbations with a non-trivial string of symmetry operations [14, 17]. In both cases, they are naturally related to the topological properties of the ground state.

In this paper, we continue this program of understanding fractionalized quasiparticles within the language of tensor networks. In the first part of the paper [Sec. I] we explain how the formalism of uniform matrix product states (MPS) gives a natural description of spinons and magnons in spin chains. Although this description confirms the received picture that spinons typically occur in half-integer spin chains, we show how they can emerge in a  $SU(2)$ -invariant spin-1 chain at a first-order transition between a symmetry-protected topological (SPT) phase and a trivial phase. In the second part [Sec. II], we provide numerical evidence for this scenario in a frustrated and dimerized spin-1 chain, and show how they are confined when tuning away from the transition.

## I. SPINONS AND MATRIX PRODUCT STATES

The formalism of translation-invariant matrix product states (MPS) in the thermodynamic limit—the so-called uniform MPS—has been developed for simulating static and dynamic properties of quantum spin chains [18]. In particular, it yields a natural description of elementary excitations as localized particles against a strongly-correlated background [19]. When implementing physical symmetries into the MPS parametrization, definite quantum numbers can be assigned to these particles [16]. In this section, we explain how this formalism is applied to  $SU(2)$  spin chains and how particles with both integer and fractional quantum numbers naturally emerge from the MPS formalism.

### A. Ground states

It is, by now, well-known that matrix product states (MPS) provide an efficient parametrization of ground states of (gapped) quantum spin chains [20, 21]. Although most state-of-the-art MPS algorithms are formulated on finite chains [22], the MPS formalism is laid out most elegantly when working in the thermodynamic limit directly [23, 24]. Indeed, a translation-invariant ground state can be represented as an MPS where we just repeat the same tensor  $A$  on each site in the chain. This can be generalized to states with larger unit cells, where we repeat the same sequence of tensors  $\{A_1, A_2, \dots\}$ . The state is represented diagrammatically as

$$|\Psi(A_1, \dots, A_n)\rangle = \dots \text{---} \boxed{A_1} \text{---} \dots \text{---} \boxed{A_n} \text{---} \dots,$$

and is translation invariant over  $n$  sites by construction. In recent years, it was shown that it is possible to variationally optimize over this set of states directly in the thermodynamic limit to find accurate ground-state approximations for a given hamiltonian [18, 25].

The real power of MPS is laid bare when imposing symmetry constraints on the tensors that reflect the physical symmetries in the system. Indeed, it has been realized that an MPS can only be invariant under certain global symmetry operations on the physical degrees of freedom if the virtual legs transform under the same symmetry [26]. Put differently, if an MPS is invariant under the global symmetry operation  $U(g) = \bigotimes_i u_i(g)$ ,

$$U(g) |\Psi(A)\rangle = |\Psi(A)\rangle, \quad \forall g,$$

it follows that the MPS tensor itself transforms as

$$\text{---} \boxed{A_i} \text{---} \text{---} \bigcirc_{u_i^g} = \text{---} \bigcirc_{V_g} \text{---} \boxed{A_i} \text{---} \bigcirc_{V_g} \text{---}.$$

In general, the representation  $V_g$  can be decomposed in a direct sum of (projective) irreps of the physical symmetry group, so that the MPS tensor decomposes into a number of blocks that are labeled by the irreps on each leg. In order for the total MPS wavefunction to transform trivially under the global symmetry operation, it is required that the tensor itself only contains non-zero blocks for which the three irreps fuse to the trivial representation—i.e., the tensor itself globally transforms trivially.

In the case of a quantum spin chain with  $SU(2)$  invariance, where the physical degrees of freedom transform under a specific spin- $s$  representation, the virtual degrees of freedom transform as a direct sum of representations of  $SU(2)$  labeled by  $j_1$  and  $j_2$ . Each block of the tensor is, therefore, labeled by three spins,

$$j_1 \text{---} \boxed{A_i} \text{---} j_2, \\ \quad \quad \quad | \\ \quad \quad \quad s$$

and is only non-zero when  $j_1$  and  $s$  can fuse to  $j_2$ .

Let us first investigate what this implies for a spin-1/2 chain. Suppose we want to write down an  $SU(2)$  invariant MPS with a one-site unit cell. Because the MPS tensor  $A$  has to transform as a singlet, we have the following condition on the allowed irreps on the bonds

$$j_1 \text{---} \boxed{A} \text{---} j_2, \\ \quad \quad \quad | \\ \quad \quad \quad s = 1/2 \quad \rightarrow |j_1 - j_2| = \frac{1}{2},$$

which implies that a half-integer  $j_1$  only couples to an integer  $j_2$ , and vice versa. If we build up an MPS using this tensor,

$$\text{---} \boxed{A}^{j_1} \text{---} \boxed{A}^{j_2} \text{---} \boxed{A}^{j_3} \text{---} \boxed{A} \text{---},$$

then this state falls apart into a sum of two states where the first state has  $j_1$  half-integer,  $j_2$  integer and so forth, and the second state contains the other representations. Therefore, for describing a singlet ground state for an  $s = 1/2$  spin chain, we need at least a two-site unit cell, where we alternate between half-integer and integer representations:

$$\text{---} \boxed{A_1}^{j_1} \boxed{A_2}^{j_2} \text{---}$$

where  $j_1$  ( $j_2$ ) only has half-integer (integer) representations, or vice versa.

This result implies that an MPS cannot describe a unique ground state of a spin-1/2 chain, a result that is closely connected to the Lieb-Schultz-Mattis theorem [27, 28], stating that a spin-1/2 chain cannot host a unique gapped ground state. Here we find that an MPS representation for a ground state necessarily breaks translation invariance, and, therefore that the translated state is an equally good ground-state approximation. The simplest example of an  $SU(2)$ -invariant MPS on a spin-1/2 chain is the Majumdar-Ghosh state [29, 30], which is obtained by interchanging  $j = 0$  and  $j = \frac{1}{2}$  representations on the virtual bonds.

The situation for integer spin chains is very different. Haldane famously showed that spin-1 chains typically have a unique ground state with a finite excitation gap [31, 32]. Using the MPS framework, it was shown that spin-1 chains host symmetry-protected topological (SPT) phases [33–35] that are characterized by a string-order parameter, spin-1/2 edge states and even degeneracies in the ground-state entanglement spectrum. The transition to a trivial phase can only occur through a phase transition. Here, the simplest example is the Affleck-Kennedy-Lieb-Tasaki state [36, 37], obtained by taking only  $j = \frac{1}{2}$  representations on the bonds.

The characteristic difference between an SPT phase and a trivial phase is again clearly seen in the MPS description of the  $SU(2)$ -invariant ground state. For a spin-1 chain, the MPS tensors necessarily have virtual repre-

sentations  $j_1$  and  $j_2$  with the property

$$\begin{array}{c} j_1 - \boxed{A_i} - j_2 \\ | \\ s = 1 \end{array} \rightarrow |j_1 - j_2| = 0, 1.$$

This implies that  $j_1$  and  $j_2$  are either both half-integer or both integer. This implies that MPS representations of ground states are possible using a one-site unit cell

$$- \boxed{A}^{j_1} - \boxed{A}^{j_2} - \boxed{A}^{j_3} - \boxed{A}^{j_4} - ,$$

where all  $j$ 's are either integer or half-integer. These two cases differentiate a trivial from an SPT phase, respectively: The degeneracies in the entanglement spectrum are determined by the multiplicities of the  $SU(2)$  representations, such that integer ones correspond to odd degeneracies and the half-integer ones to even degeneracies.

## B. Elementary excitations

Besides ground states, the uniform MPS framework can be extended to the description of elementary excitations. Indeed, it was rigorously shown that an excitation that lives on an isolated branch in the spectrum can be described by acting with a momentum superposition of a local operator onto the ground state [38]. In the MPS language, this translates to a quasiparticle ansatz for elementary excitations on top of an MPS ground state [39]. When applied to an  $SU(2)$  invariant spin system with a unique translation-invariant ground state, we have the following form for an elementary excitation

$$|\Phi_p^k(B)\rangle = \sum_n e^{ipn} - \boxed{A}^{j_1}_{s_{n-2}} - \boxed{A}^{j_2}_{s_{n-1}} - \boxed{B}^k_{s_n} - \boxed{A}^{j_3}_{s_{n+1}} - \boxed{A}^{j_4}_{s_{n+2}} - .$$

Here we have introduced a new tensor  $B$  that perturbs the ground state in a local region around site  $n$ , and performed a plane-wave superposition with momentum  $p$ . We have added an extra leg to this tensor that transforms according to a certain  $SU(2)$  irrep, labeled by  $k$ . Therefore, the irrep that lives on this non-contracted leg determines the global quantum number of the excited state.

The ansatz wavefunction is linear in the tensor  $B$ , and therefore the variational parameters in  $B$  can be optimized by solving a generalized eigenvalue problem. Using a specific parametrization for the tensor  $B$ , the norm of the wavefunction can be made trivial, which reduces the generalized eigenvalue problem to an ordinary one. When the quantum numbers of the excitation—the momentum  $p$  and the  $SU(2)$  label  $k$ —are non-trivial, the excitation is orthogonal to the ground state by construction; for trivial quantum numbers the ansatz can be made orthogonal by the same parametrization.

It is easily seen that when considering integer-spin chains, regardless of whether the  $j$ 's are integer or half-integer, the label  $k$  has to be an integer. This corresponds to the well-known property that spin-1 chains generically have magnon excitations.

In the half-integer spin case, where the MPS breaks translation invariance and has a two-site unit cell, we can make elementary excitations by considering defects in the ground-state pattern. Indeed, an excitation would look like

$$|\Phi_p^k(B)\rangle = \sum_n e^{ipn} - \boxed{A_1}^{j_e}_{s_{n-2}} - \boxed{A_2}^{j_o}_{s_{n-1}} - \boxed{B}^k_{s_n} - \boxed{A_1}^{j_o}_{s_{n+1}} - \boxed{A_2}^{j_e}_{s_{n+2}} - .$$

One now observes that the label  $k$  has to be half-integer, which indicates that elementary excitations in spin-1/2 chains generically have half-integer quantum numbers. These spinons cannot be created out of the ground state by a local operator, but are always created in pairs; this phenomenon is known as fractionalization.

From the MPS perspective, therefore, it is natural that half-integer spin chains host spinon excitations, whereas magnons appear in integer-spin chains. There is, however, a scenario conceivable where spinon excitations can emerge in a spin-1 chain. We imagine that we tune the system such that there is a coexistence of two MPS ground states  $|\Psi(A_1)\rangle$  and  $|\Psi(A_2)\rangle$ , where one MPS carries only integer representations on the legs and the other only half-integer ones. Put differently, we require that the system is at a first-order transition between an SPT phase and a trivial phase. In that case, we can consider solitonic excitations between the two ground states,

$$|\Phi_p^k(B)\rangle = \sum_n e^{ipn} - \boxed{A_1}^{j_e}_{s_{n-2}} - \boxed{A_1}^{j_e}_{s_{n-1}} - \boxed{B}^k_{s_n} - \boxed{A_2}^{j_o}_{s_{n+1}} - \boxed{A_2}^{j_o}_{s_{n+2}} - .$$

It is easily seen now that the irrep label  $k$  has to be half-integer, so it carries fractional quantum numbers.

## C. Spinon/anti-spinon bound states

Spin chains that host spinon excitations can often be perturbed such that the spinons are confined. In the above case of spin-1/2 chains, the easiest option is to favour one of the two ground-state patterns through an explicit dimerization in the spin-chain hamiltonian. In that case, the spinons no longer exist as elementary excitations, but if the perturbation is weak, one can still understand the low-lying excitations as spinon/anti-spinon bound states. These can be pictured as consisting of two local kinks in the ground state pattern, and can be de-

scribed by a two-particle wavefunction of the form

$$|\Phi_p^k(B)\rangle = \sum_n e^{ipn} \sum_{n' > 0, \text{even}} c(n')$$

where  $c(n')$  is the part of the two-particle wavefunction for the relative position between the two spinons.

In the case of spinons in a spin-1 chain at a first-order transition line, a spinon/anti-spinon wavefunction would look like

$$|\Phi_p^k(B)\rangle = \sum_n e^{ipn} \sum_{n' > 0} c(n')$$

Here spinon confinement can be easily introduced by tuning slightly away from the first-order point such that one of the two ground states is favoured over the other energetically.

This type ansatz wavefunction was introduced for describing two-particle scattering states [19, 40], for which the relative wavefunction  $c(n')$  has an oscillating form. It was shown in Ref. [15] that the transition of a scattering state into a bound state corresponds to the relative wavefunction  $c(n)$  changing from an oscillating function into an exponentially decaying one. This process of bound-state formation is signalled in the divergence of the scattering length, which can be read off from  $c(n)$  [15].

In principle, however, the description of stable bound states fall within the above one-particle framework: their wavefunctions are constructed as local deformations of the ground state in a momentum superpositions. Indeed, for strongly-bound states, the one-particle ansatz has proven to be sufficient to capture the wavefunction accurately [15, 41]. However, when very broad bound states are considered—when the two  $B$  tensors are separated—the above quasiparticle ansatz can be insufficient in the sense that a single local tensor cannot capture the full extension of the ground-state perturbation. In that case, an extended ansatz of the form [38]

$$|\Phi_p^k(B)\rangle = \sum_n e^{ipn} \text{---} [A] \text{---} [B] \text{---} [A] \text{---}$$

can be introduced. The number of parameters in the  $B$  tensor scales exponentially with the number of sites  $N$ , such that a variational optimization becomes unfeasible rather quickly. For that reason, we can decompose the  $B$  tensor in a string of  $N$  one-site tensors giving rise to the

ansatz

$$|\Phi_p^k(B)\rangle = \sum_n e^{ipn} \text{---} [A] \text{---} [B_1] \text{---} [B_2] \text{---} \dots \text{---} [B_N] \text{---} [A] \text{---}$$

The variational optimization of the string of tensors can be performed using a sweeping algorithm, much in the spirit of standard DMRG [22] algorithms—we refer to the appendix for more details on the implementation.

## II. SPINONS AND THEIR CONFINEMENT IN THE SPIN-1 CHAIN

The MPS formalism allows to capture generic cases of spinons and their confinement in  $SU(2)$ -invariant spin chains. In addition, we have proposed the scenario in which spin-1/2 spinons can emerge in a spin-1 chain on a first-order transition line. This phenomenon was observed to occur in a frustrated and dimerized spin-1 chain [42]—the spin-1 chain with next-nearest neighbour and biquadratic interactions shows a similar phenomenology [43, 44]. In this section we apply our formalism to the former model. In addition, we study the confinement of these spinons away from the transition line. In Refs. 15 and 41 spinon confinement in spin-1/2 chains was already simulated using the framework of uniform MPS without symmetries. In the following we have performed the simulations using tangent-space methods for uniform MPS [18] using full  $SU(2)$ -symmetric tensor-network operations [45].

### A. Spinons on a first-order transition line

We investigate the frustrated and dimerized spin-1 chain, defined by the hamiltonian

$$H = J_1 \sum_i \vec{S}_i \cdot \vec{S}_{i+1} + J_2 \sum_i \vec{S}_{i-1} \cdot \vec{S}_{i+1} + J_3 \sum_i \left( (\vec{S}_{i-1} \cdot \vec{S}_i)(\vec{S}_i \cdot \vec{S}_{i+1}) + h.c. \right).$$

For  $J_2 = J_3 = 0$  this model reduces to the spin-1 Heisenberg model, which is known to be in the Haldane phase [31, 32]. The next-nearest neighbour term ( $J_2$ ) adds frustration to the system and drives it through a first-order phase transition into a trivial phase [46, 47], whereas the three-site interaction ( $J_3$ ) induces a spontaneous dimerization via a second-order transition [48]. The full phase diagram (see Fig. 1) shows that the first-order transition extends over a finite region, and only for small  $J_2$  the transition into the dimerized phase becomes second order.

Let us first investigate the first-order transition between the SPT phase and the trivial phase. On both sides of the transition, we can represent the ground state

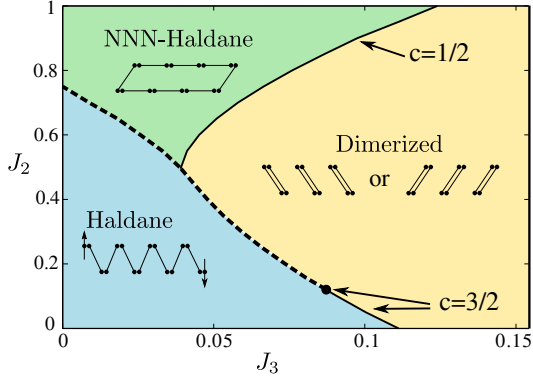


FIG. 1. The phase diagram of the frustrated and dimerized spin-1 chain, taken from Ref. 42. The three phases are pictorially represented by a picture of virtual spin-1/2 particles: the SPT phase is a Haldane phase, the trivial phase can be interpreted as a next-nearest-neighbour Haldane phase, and in the dimerized phase the pairing of the virtual particles leads to a spontaneous breaking of translation symmetry. The full (dashed) lines represent second-order (first-order) transitions.

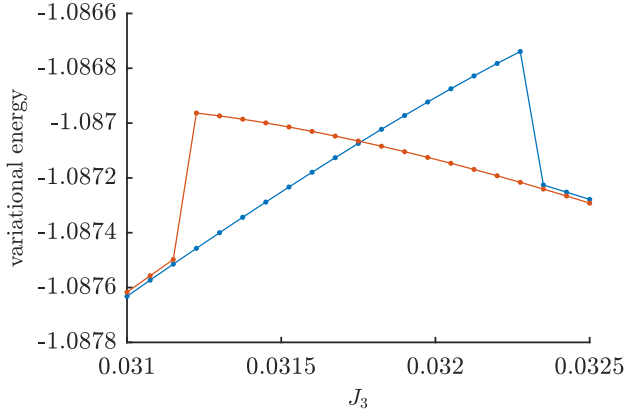


FIG. 2. The variational energy obtained by MPS with half-integer (blue) and integer (red) representations on the links for  $J_1 = 1$ ,  $J_2 = 0.56$ , and as a function of  $J_3$ . We observe a crossing indicating a first-order transition between an SPT phase and a trivial phase. The blue (red) data points were obtained by taking the previous MPS as the starting point for the next point, such that the vumps algorithm stays in the local minimum corresponding to the higher-energy state. Ultimately, the variational optimization drops farther away from the phase transition, where the MPS with the wrong representations will develop a non-injective structure to approximate the true ground state.

by an MPS with a one-site unit cell with an explicit encoding of the SU(2) symmetry: In the SPT phase, we choose half-integer representations on the virtual degrees of freedom, whereas in the trivial phase we choose only the integer ones. Because these two choices determine different classes of MPS, we can compare the variational energies within the two distinct classes and determine in which phase the ground state is for a given choice of pa-

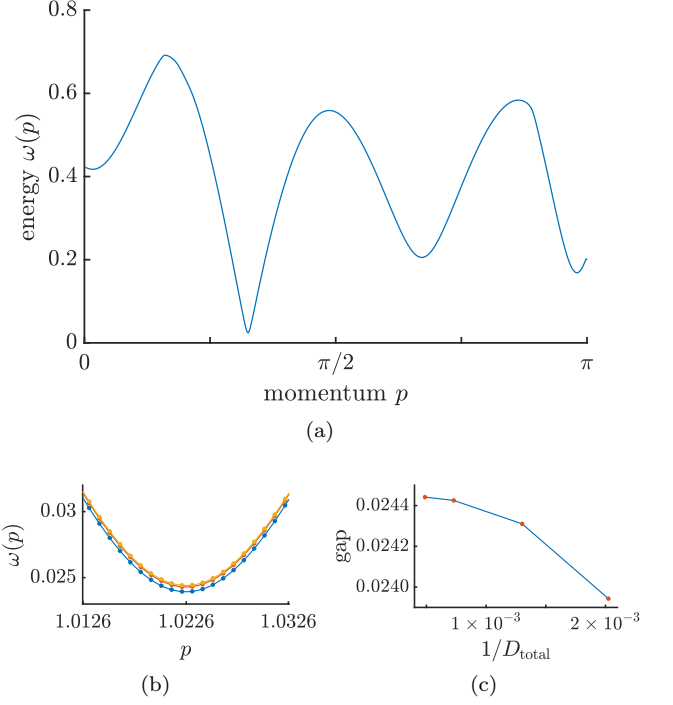


FIG. 3. In (a) we plot the dispersion relation of the spinon excitation at the first-order phase transition between Haldane and trivial phase at  $J_2 = 0.56$ ,  $J_3 \approx 0.0318$ . The full dispersion relation has been computed using the spinon quasi-particle ansatz with SU(2) symmetry. To get an idea for the convergence as a function of bond dimension, in (b) and (c) we plot the dispersion around the minimum and the convergence of the gap with higher bond dimensions (up to  $D = 200$  for the largest subblock; for comparison, this corresponds to a non-symmetric MPS with total bond dimension  $D_{\text{total}} \approx 2000$ ). Note that the excitation energy is not variational, because we subtract the MPS ground-state energy.

rameters. In Fig. 2 we plot the variational energies on a line in the phase diagram that crosses the transition, showing nicely that this is, indeed, a first-order transition.

Exactly at the transition, the two ground states have the same energy density. Therefore, we can consider domain walls that interpolate between them, where, as we have shown in the previous section, the excitations necessarily carry a half-integer quantum number. In Fig. 3 we plot the dispersion relation of the spinons with spin  $s = 1/2$  for  $J_2 = 0.56$  and  $J_3 \approx 0.0318$ . The spinon's dispersion relation exhibits a very strong minimum at an incommensurate value of the momentum. In the inset, we provide a close-up around the minimum showing that the gap converges to a non-zero value. In addition, in Fig. 4 we plot the dispersion relation further along the transition line ( $J_2 \approx 0.7606$ ,  $J_3 = 0$ ) showing that the spinon gap decreases. It is expected that the gap ultimately closes when going further along this line—this closing of the gap can be described by a marginal operator chang-



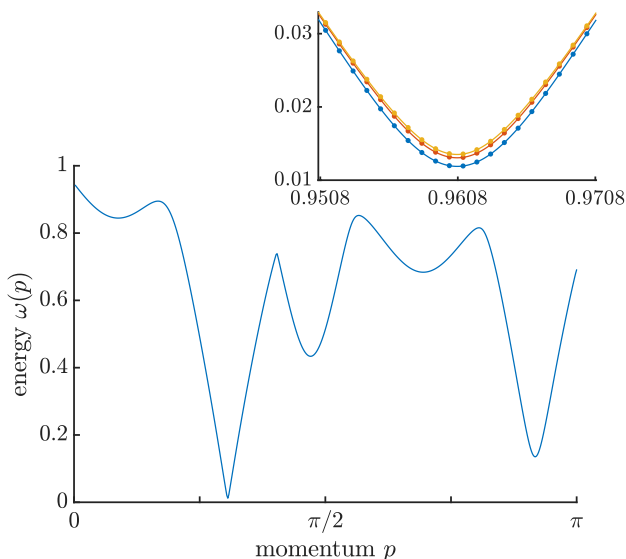


FIG. 4. The same plot as before, now for parameters  $J_2 \approx 0.7606$  and  $J_3 = 0$ . The inset shows that the spinon has decreased significantly with respect to the previous figure.

ing sign in the  $SU(2)_1$  Wess-Zumino-Witten field theory with central charge  $c = 1$  [49, 50]. A continuous transition with  $c = 1$  between an SPT chain and a trivial phase was recently demonstrated in Ref. 51. Unfortunately, we have found no immediate evidence for a critical point further along the transition line, and we leave an elaborate study of this question for further work.

The existence of the spinons as low-energy excitations at the phase transitions can be further confirmed from simulations on a finite chain [42]. The SPT phase is known to have symmetry-protected spin-1/2 edge states localized at the end of the corresponding domain. Therefore a domain wall between an SPT phase and a topologically trivial phase, either NNN-Haldane or dimerized, necessarily carries a spin-1/2. At the first order transition the energy levels of the corresponding states cross and one can observe the coexistence of different domains. In Fig. 5 we show the results at the first-order transition between the topologically trivial and SPT phases at  $J_2 = 0.75$ ,  $J_3 \approx 0$ . Four quantities are the most relevant: the local magnetization  $\langle S_j^z \rangle$  that reveals the spin-1/2 domain wall; the nearest neighbor correlations, which reflects the presence of the dimerization in the domain; the three-site correlations that signals the SPT phase when it is large and positive; and the bipartite entanglement entropy  $EE_N$  that takes its maximal value at the domain wall. According to Fig. 5(c) open edges favor topologically trivial domains, while the central domain is in the Haldane phase. Although the local magnetization profile shown in Fig. 5(a) is significantly perturbed by incommensurate correlations, one can clearly see that the maximum of the amplitude is shifted away from the boundary. According to the entanglement entropy profile shown in Fig. 5(d) spin-1/2 domain walls are approximately 30

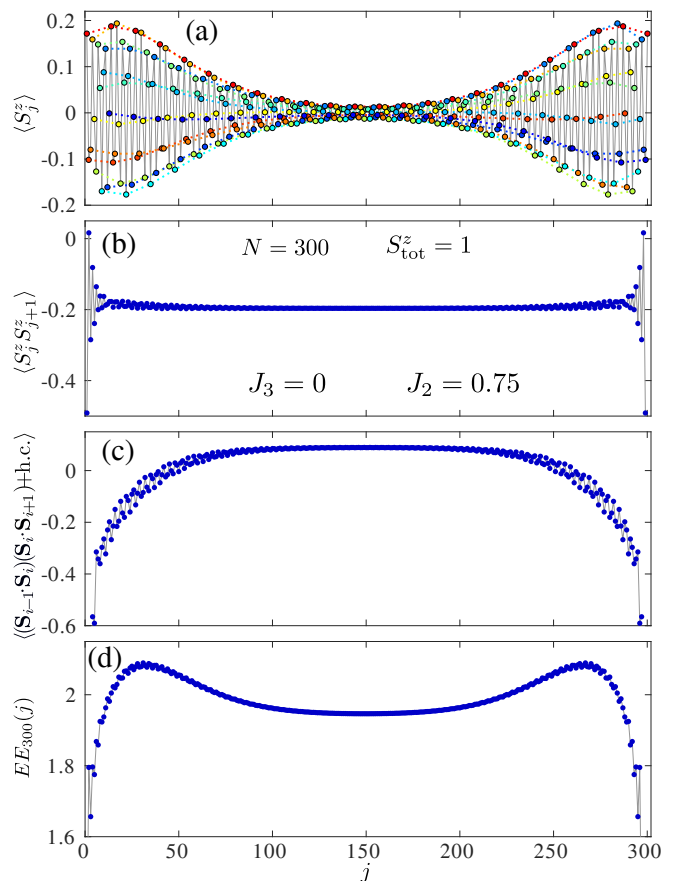


FIG. 5. (a) Local magnetization, (b) nearest-neighbour correlations, (c) three-site correlations, and (d) bipartite entanglement profile for a chain with  $N = 300$  sites and  $S_{\text{tot}}^z = 1$  at the first-order transition between the SPT and trivial phase at  $J_2 \approx 0.75$  and  $J_3 = 0$ .

sites away from the edges, which agrees with the local magnetization profile.

We have also studied the first-order transition between the SPT phase and the dimerized phase for smaller  $J_2$ . The situation is slightly more complicated, because the dimerized phase itself hosts spinon excitations as well. Indeed, the dimerized phase has an MPS ground-state description with a two-tensor unit cell, and the low-energy particles are spin-1 defects in the ground-state pattern. In order to focus on the spin-1/2 spinons around the phase transition, we perform a blocking transformation such that a dimerized ground state maps to a translation-invariant MPS described by a single tensor with integer  $SU(2)$  representations on the virtual bonds. In this setting, the description of the spinons on the first-order transition line is similar as before.

For this case, it is known [49] that the first-order line ends and becomes second order, where the transition is described by a  $SU(2)_2$  Wess-Zumino Witten field theory with central charge  $c=3/2$ . The transition between first and second order—i.e., the closing of the spinon gap as one travels on the phase-transition line—is described by

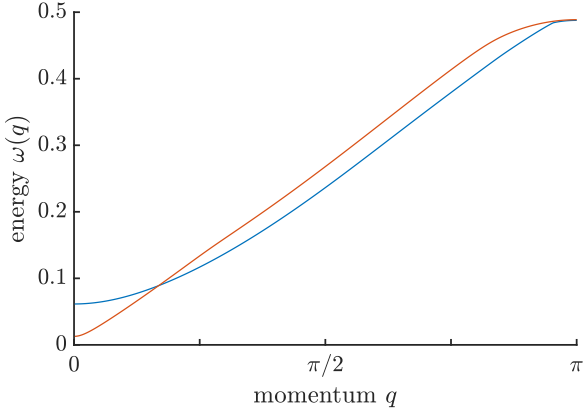


FIG. 6. The spinon dispersion relation on the first-order transition line between the SPT phase and the dimerized phase, for parameters  $(J_2, J_3)$  given by  $(0.3265, 0.0558)$  (blue) and  $(0.2915, 0.0603)$ . The dimerized ground state breaks one-site translation invariance spontaneously, so the momentum  $q$  is defined with respect to translations over two sites.

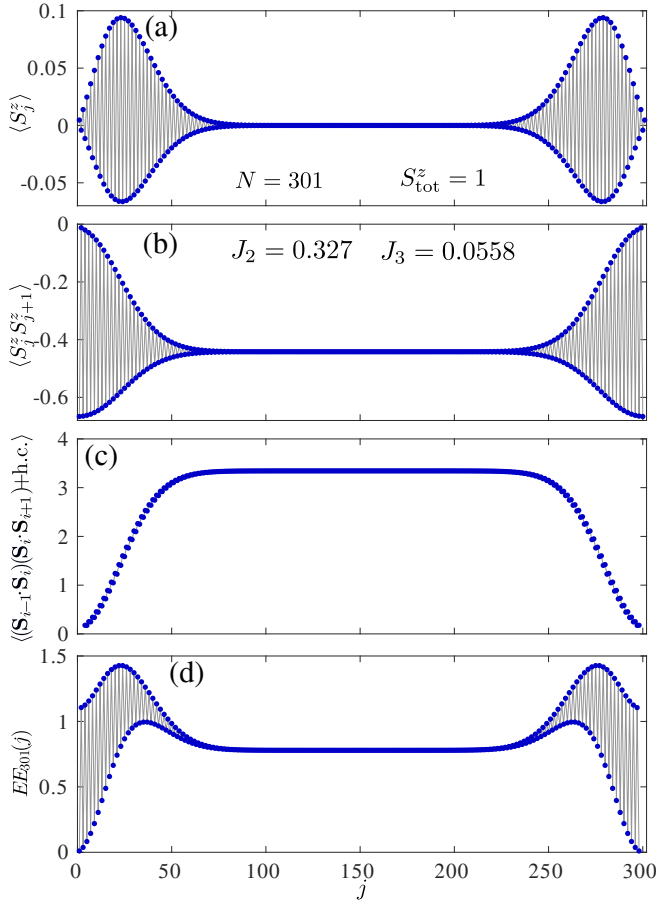


FIG. 7. (a) Local magnetization, (b) nearest-neighbour correlations, (c) three-site correlations, and (d) bipartite entanglement profile for a chain of  $N = 301$  sites and  $S_{\text{tot}}^z = 1$  at the first-order transition between the SPT and dimerized phase at  $J_2 = 0.327$  and  $J_3 = 0.0558$ .

a marginal operator in the field theory changing sign.

In Fig. 6 we plot the spinon dispersion relation for two points on the first-order transition line between SPT and dimerized phase. First we observe that the minimum of the dispersion relation is at momentum  $q = 0$ , so we do not have any commensurate correlations in the system. Moreover, we observe that the spinon gap becomes smaller quickly as we travel on the transition line towards the critical point. This rapid decrease of the gap is expected from the field-theory description, which predicts an exponential suppression as the critical point is approached.

In the present case we also confirm the existence of the spinons by looking at four finite-size profiles listed above. The calculations have been done for the lowest energy state in the sector with  $S_{\text{tot}}^z = 1$  and  $N = 301$ . Based on Figs. 7(a), (b) and (c) one can deduce that open edges favor dimerized domains, while the central region remains in the SPT phase. Note, however, that for a selected coupling constant the SPT domain is still commensurate, which implies that the ground-state is a singlet if the total number of sites is even, and the ground-state is a (Kennedy) triplet [52], if the total size of the domain is odd. Moreover, the dimerized domains necessary contain an even number of sites. So, keeping the total number of sites odd, we ensure a Kennedy triplet on the central SPT domain. According to Fig. 7(a) the domain walls are located at a distance about 25 spins from each edge, and the entanglement entropy also takes its maximal values at these locations.

## B. Confinement of spinons around the transition line

The spinons that we have identified in the previous section exist as freely propagating particles only at the first-order phase transition exactly, but their existence has noticeable effect away from the transition as well. Indeed, we imagine that both ground states still exist independently away from the transition point, where one of the two will have slightly lower energy density (see Fig. 2). As we have explained in Sec. IC, we can still consider spinon/anti-spinon pairs against the background of the ground state that is favoured energetically. The excess of energy between the spinon and anti-spinon due to the higher-energy background state between them causes the spinon/anti-spinon pair to experience a linear potential and form bound states. As discussed in the introduction, this phenomenon has been studied extensively in spin-1/2 chains [8–11, 15, 41].

The formation of spinon/anti-spinon bound states away from the first-order phase transition is observed when plotting the excitation spectrum for a few values of the coupling inside the Haldane phase, see Fig. 8. Indeed, for  $J_2 = J_3 = 0$  we find the usual spectrum of the Heisenberg chain with a minimum in the dispersion at momentum  $\pi$ . When we come closer to the phase

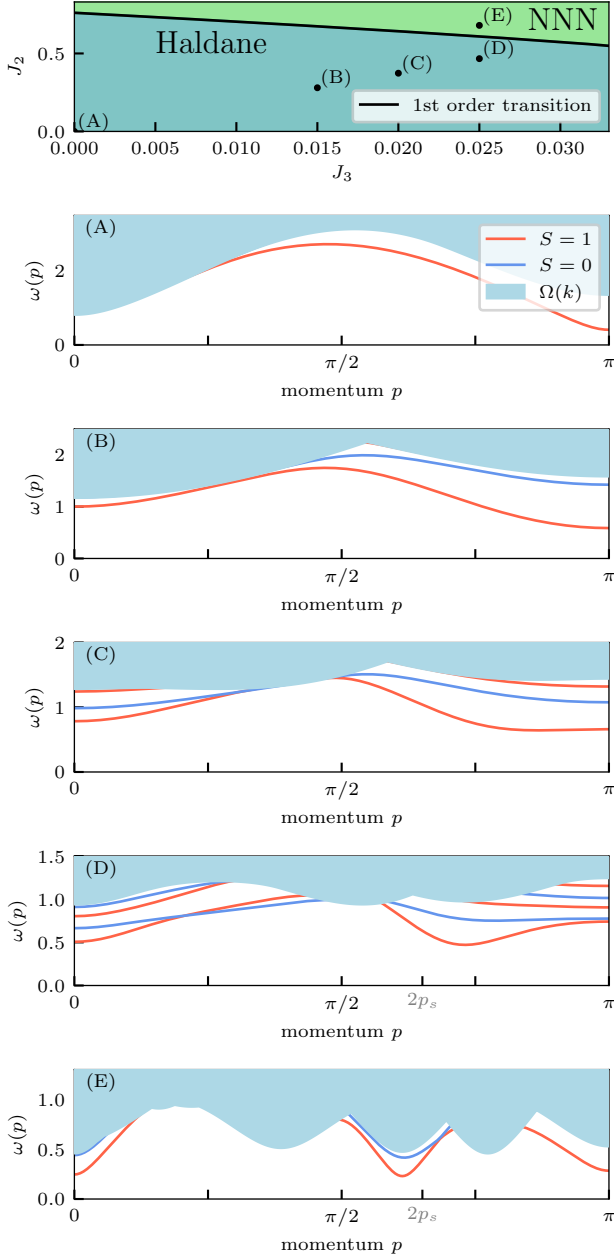


FIG. 8. Excitation spectra for different points in the phase diagram. The blue shaded areas are multi-particle continua, the lines are the first low-lying spin-0 and spin-1 excitations. We observe an accumulation of bound-state modes in the spectrum as the first-order transition is approached. The third spectrum also shows the formation of an incommensurate minimum. The extra tick in grey shows twice the momentum for which the spinon dispersion relation is minimal, see Fig. 3. The simulations were performed at bond dimension  $D_{\text{total}} = 120$ .

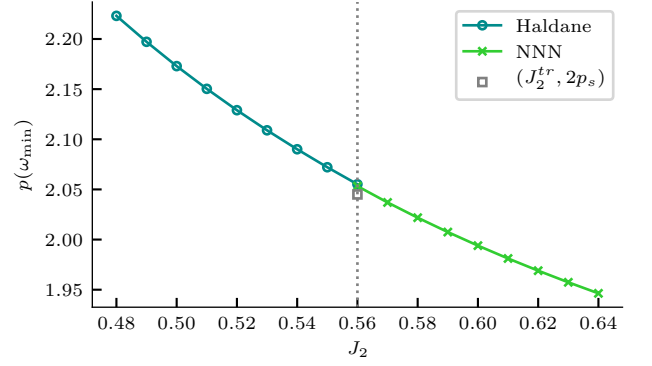


FIG. 9. The momentum for which the dispersion relation reaches its minimum at  $J_3 = 0.0318$  as a function of  $J_2$ . At  $J_2 \approx 0.56$  the system undergoes a first-order phase transition. The value of  $p(\omega_{\min})$  is then compatible with two times the momentum of the gap in the free spinon dispersion relation (see Fig. 3,  $p_s \approx 1.0226$ ) as indicated by the grey square. The simulations were performed at bond dimension  $D_{\text{total}} = 120$ .

transition, we find that the minimum starts shifting to an incommensurate value, an observation that was also made from the real-space correlation functions [42]. More interestingly, we find different isolated lines below the continuum emerging when approaching the phase transition. The minima of these isolated lines are situated at momentum  $p = 0$  and at an incommensurate value  $p = p_{\text{inc}}$ . Above we have seen that the spinon dispersion relation has a strong minimum at momentum  $p_s$ , so that we expect, indeed, to see bound states around momenta  $p = p_s \pm p_s$ .

In Fig. 9 we have explicitly tracked the behavior of these incommensurate values. We varied  $J_2$  at constant  $J_3$  towards the first order transition point. From both the Haldane phase and the NNN-trivial phase, we indeed observe convergence towards  $p = 2p_s$  which confirms the confinement of the spinons away from the transition line.

In addition we have applied the extended quasiparticle ansatz for broad bound states, containing a string of tensors [Sec. IC]. In Fig. 10 we show the performance of this extended ansatz for the lowest-lying excitation in the system upon approaching the phase transition. When far away from the transition, the variational energy converges very quickly, which shows that the bound state has a limited spatial extent. If the transition is approached, the convergence becomes slower, which points to a widening of the spinon/anti-spinon bound state. The fact that the excitations become broad, extended perturbations of the ground state as the first-order transition is approached, confirms our underlying spinon picture for the low-lying excitations in the vicinity of the first-order phase transition.



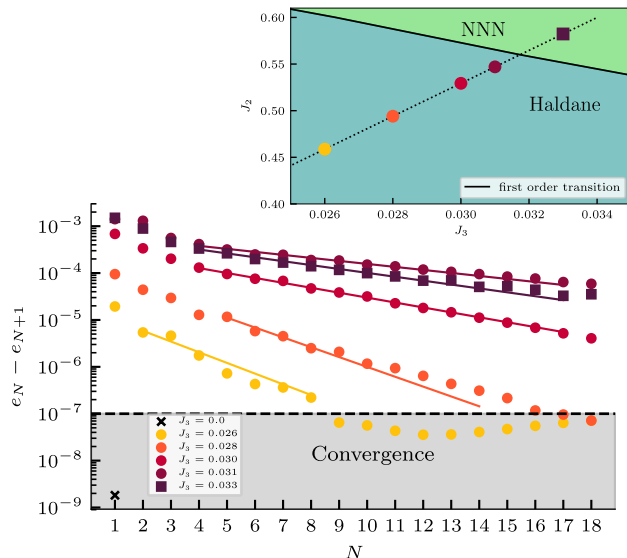


FIG. 10. The convergence of the variational excitation energies at momentum  $k = 0$  as a function of the spatial support  $N$  of the string ansatz at various points near the phase transition (bottom). These points are located on the line through the origin and the transition point  $J_2 = 0.56, J_3 \approx 0.0318$  (top). The convergence becomes better further away from the phase transition, which is consistent with the bound state picture. For comparison we show the convergence of the magnon (with  $k = \pi$ ) at the Heisenberg point  $J_2 = 0, J_3 = 0$  (black cross).

### III. CONCLUSIONS

In the first part of this paper we laid out the formalism of MPS for describing ground states and elementary excitations of  $SU(2)$  invariant spin chains, showing how fractionalized spinons emerge naturally from the symmetry pattern of the ground-state MPS tensors. The same

analysis can be extended to chains with other global symmetries, where the case of  $SU(N)$  is arguably the most interesting. For example, a three-tensor ground state naturally appears for a  $SU(3)$  chain in the fundamental representation, and one can consider two types of defects or spinons against this background.

In two dimensions, the framework of projected entangled-pair states (PEPS) allows to simulate even more exotic quasiparticles [53, 54]. Indeed, whereas the one-dimensional case only allows for defects in the ground-state pattern, in two dimensions we can consider quasiparticles with non-trivial strings of symmetry operations as well [17, 35]. An  $SU(2)$ -symmetric PEPS both hosts spinons and visons as elementary excitations [55], and it would be interesting to study these quasiparticles and their confinement for spin-liquid hamiltonians.

Spinon excitations have been observed in neutron-scattering experiments on quasi-one-dimensional compounds [56–60]. The fact that the spinons necessarily come in pairs leads to a broad continuum in the dynamical structure factor, in contrast to the more conventional magnon mode. In more recent neutron-scattering experiments, the confinement of these particles has been observed by the splitting of the multi-spinon continuum into a stack of bound states [41, 61]. In this work, we have shown that spinon confinement is generic at first-order transitions between SPT and trivial phases in spin-1 chains, so it would be very interesting if this effect can be observed experimentally as well.

We acknowledge insightful discussions with Ian Affleck about solitons in spin chains. This research is supported by the Research Foundation Flanders (LV, FV), the Swiss National Science Foundation (NC, FM), the German Research Foundation (Deutsche Forschungsgemeinschaft, DFG) through TRR80 Project F8 (EW), and ERC grant QUTE (FV).

- 
- [1] L. D. Faddeev and L. A. Takhtajan, What is the spin of a spin wave?, *Physics Letters A* **85**, 375 (1981).
  - [2] L. D. Faddeev and L. A. Takhtajan, Spectrum and scattering of excitations in the one-dimensional isotropic Heisenberg model, *Journal of Mathematical Sciences* (1984).
  - [3] J. des Cloizeaux and J. J. Pearson, Spin-Wave Spectrum of the Antiferromagnetic Linear Chain, *Physical Review* **128**, 2131 (1962).
  - [4] F. D. M. Haldane, Exact jastrow-gutzwiller resonating-valence-bond ground state of the spin-1/2 antiferromagnetic heisenberg chain with  $1/r^2$  exchange, *Physical Review Letters* **60**, 635 (1988).
  - [5] F. D. M. Haldane, “spinon gas” description of the  $s=1/2$  heisenberg chain with inverse-square exchange: Exact spectrum and thermodynamics, *Physical Review Letters* **66**, 1529 (1991).
  - [6] B. S. Shastry and B. Sutherland, Excitation spectrum of a dimerized next-neighbor antiferromagnetic chain, *Physical Review Letters* **47**, 964 (1981).
  - [7] W. P. Su, J. R. Schrieffer, and A. J. Heeger, Solitons in polyacetylene, *Physical Review Letters* **42**, 1698 (1979).
  - [8] E. Sørensen, I. Affleck, D. Augier, and D. Poilblanc, Soliton approach to spin-peierls antiferromagnets: Large-scale numerical results, *Physical Review B* **58**, R14701 (1998).
  - [9] I. Affleck, Soliton Confinement and the Excitation Spectrum of Spin-Peierls Antiferromagnets, in *Dynamical Properties of Unconventional Magnetic Systems SE - 6*, NATO ASI Series, Vol. 349, edited by A. Skjeltorp and D. Sherrington (Springer Netherlands, 1998) pp. 123–131.
  - [10] D. Augier, E. Sørensen, J. Riera, and D. Poilblanc, Soliton bound states in the Raman spectrum of pure and doped spin-Peierls chains, *Physical Review B* **60**, 1075 (1999).
  - [11] H. Shiba, Quantization of magnetic excitation continuum due to interchain coupling in nearly one-

- dimensional ising-like antiferromagnets, *Progress of Theoretical Physics* **64**, 466 (1980).
- [12] M. Kormos, M. Collura, G. Takács, and P. Calabrese, Real-time confinement following a quantum quench to a non-integrable model, *Nature Physics* **13**, 246 (2017).
  - [13] F. Liu, R. Lundgren, P. Titum, G. Pagano, J. Zhang, C. Monroe, and A. V. Gorshkov, Confined quasiparticle dynamics in long-range interacting quantum spin chains, *Physical Review Letters* **122**, 150601 (2019).
  - [14] N. Schuch, J. I. Cirac, and D. Pérez-García, Peps as ground states: Degeneracy and topology, *Annals of Physics* **325**, 2153 (2010).
  - [15] L. Vanderstraeten, J. Haegeman, F. Verstraete, and D. Poilblanc, Quasiparticle interactions in frustrated heisenberg chains, *Physical Review B* **93**, 235108 (2016).
  - [16] V. Zauner-Stauber, L. Vanderstraeten, J. Haegeman, I. P. McCulloch, and F. Verstraete, Topological nature of spinons and holons: Elementary excitations from matrix product states with conserved symmetries, *Physical Review B* **97**, 235155 (2018).
  - [17] J. Haegeman, V. Zauner, N. Schuch, and F. Verstraete, Shadows of anyons and the entanglement structure of topological phases, *Nature Communications* **6**, 8284 (2015).
  - [18] L. Vanderstraeten, J. Haegeman, and F. Verstraete, Tangent-space methods for uniform matrix product states, *SciPost Physics Lecture Notes*, 7 (2019).
  - [19] L. Vanderstraeten, F. Verstraete, and J. Haegeman, Scattering particles in quantum spin chains, *Physical Review B* **92**, 125136 (2015).
  - [20] M. B. Hastings and T. Koma, Spectral gap and exponential decay of correlations, *Communications in Mathematical Physics* **265**, 781 (2006).
  - [21] F. Verstraete and J. I. Cirac, Matrix product states represent ground states faithfully, *Physical Review B* **73**, 094423 (2006).
  - [22] U. Schollwöck, The density-matrix renormalization group in the age of matrix product states, *Annals of Physics* **326**, 96 (2011).
  - [23] G. Vidal, Classical simulation of infinite-size quantum lattice systems in one spatial dimension, *Physical Review Letters* **98**, 070201 (2007).
  - [24] J. Haegeman, J. I. Cirac, T. J. Osborne, I. Pizorn, H. Verschelde, and F. Verstraete, Time-dependent variational principle for quantum lattices, *Physical Review Letters* **107**, 070601 (2011).
  - [25] V. Zauner-Stauber, L. Vanderstraeten, M. T. Fishman, F. Verstraete, and J. Haegeman, Variational optimization algorithms for uniform matrix product states, *Physical Review B* **97**, 045145 (2018).
  - [26] D. Pérez-García, F. Verstraete, M. M. Wolf, and J. I. Cirac, Matrix product state representations, arXiv (2006), [quant-ph/0608197](https://arxiv.org/abs/quant-ph/0608197).
  - [27] E. H. Lieb, T. Schultz, and D. Mattis, Two soluble models of an antiferromagnetic chain, *Annals of Physics* **16**, 407 (1961).
  - [28] M. Oshikawa, Commensurability, excitation gap, and topology in quantum many-particle systems on a periodic lattice, *Physical Review Letters* **84**, 1535 (2000).
  - [29] C. K. Majumdar and D. K. Ghosh, On nextnearestneighbor interaction in linear chain. i, *Journal of Mathematical Physics* **10**, 1388 (1969).
  - [30] C. K. Majumdar and D. K. Ghosh, On nextnearestneighbor interaction in linear chain. ii, *Journal of Mathematical Physics* **10**, 1399 (1969).
  - [31] F. D. M. Haldane, Continuum dynamics of the 1-d heisenberg antiferromagnet: Identification with the o(3) nonlinear sigma model, *Physics Letters A* **93**, 464 (1983).
  - [32] F. D. M. Haldane, Nonlinear field theory of large-spin heisenberg antiferromagnets: Semiclassically quantized solitons of the one-dimensional easy-axis néel state, *Physical Review Letters* **50**, 1153 (1983).
  - [33] F. Pollmann, A. M. Turner, E. Berg, and M. Oshikawa, Entanglement spectrum of a topological phase in one dimension, *Physical Review B* **81**, 064439 (2010).
  - [34] X. Chen, Z.-C. Gu, and X.-G. Wen, Classification of gapped symmetric phases in one-dimensional spin systems, *Physical Review B* **83**, 035107 (2011).
  - [35] N. Schuch, D. Pérez-García, and J. I. Cirac, Classifying quantum phases using matrix product states and projected entangled pair states, *Physical Review B* **84**, 165139 (2011).
  - [36] I. Affleck, T. Kennedy, E. H. Lieb, and H. Tasaki, Rigorous results on valence-bond ground states in antiferromagnets, *Physical Review Letters* **59**, 799 (1987).
  - [37] I. Affleck, T. Kennedy, E. H. Lieb, and H. Tasaki, Valence bond ground states in isotropic quantum antiferromagnets, *Communications in Mathematical Physics* **115**, 477 (1988).
  - [38] J. Haegeman, S. Michalakis, B. Nachtergaele, T. J. Osborne, N. Schuch, and F. Verstraete, Elementary excitations in gapped quantum spin systems, *Physical Review Letters* **111**, 080401 (2013).
  - [39] J. Haegeman, B. Pirvu, D. J. Weir, J. I. Cirac, T. J. Osborne, H. Verschelde, and F. Verstraete, Variational matrix product ansatz for dispersion relations, *Physical Review B* **85**, 100408 (2012).
  - [40] L. Vanderstraeten, J. Haegeman, T. J. Osborne, and F. Verstraete, *s* matrix from matrix product states, *Physical Review Letters* **112**, 257202 (2014).
  - [41] A. K. Bera, B. Lake, F. H. L. Essler, L. Vanderstraeten, C. Hubig, U. Schollwöck, A. T. M. N. Islam, A. Schneidewind, and D. L. Quintero-Castro, Spinon confinement in a quasi-one-dimensional anisotropic heisenberg magnet, *Physical Review B* **96**, 054423 (2017).
  - [42] N. Chepiga, I. Affleck, and F. Mila, Spontaneous dimerization, critical lines, and short-range correlations in a frustrated spin-1 chain, *Physical Review B* **94**, 205112 (2016).
  - [43] J. H. Pixley, A. Shashi, and A. H. Nevidomskyy, Frustration and multicriticality in the antiferromagnetic spin-1 chain, *Physical Review B* **90**, 214426 (2014).
  - [44] N. Chepiga, I. Affleck, and F. Mila, Comment on “frustration and multicriticality in the antiferromagnetic spin-1 chain”, *Physical Review B* **94**, 136401 (2016).
  - [45] B. Vanhecke, et. al., Implementation of non-abelian symmetric tensor-network operations, *in preparation*.
  - [46] A. Kolezhuk, R. Roth, and U. Schollwöck, First order transition in the frustrated antiferromagnetic heisenberg  $s = 1$  quantum spin chain, *Physical Review Letters* **77**, 5142 (1996).
  - [47] A. Kolezhuk, R. Roth, and U. Schollwöck, Variational and density-matrix renormalization-group studies of the frustrated antiferromagnetic heisenberg  $s=1$  quantum spin chain, *Physical Review B* **55**, 8928 (1997).
  - [48] F. Michaud, F. Vernay, S. R. Manmana, and F. Mila, Antiferromagnetic spin- $s$  chains with exactly dimerized ground states, *Physical Review Letters* **108**, 127202 (2012).

- (2012).
- [49] N. Chepiga, I. Affleck, and F. Mila, Dimerization transitions in spin-1 chains, *Physical Review B* **93**, 241108 (2016).
  - [50] L. Tsui, Y.-T. Huang, H.-C. Jiang, and D.-H. Lee, The phase transitions between znzn bosonic topological phases in 1+1d, and a constraint on the central charge for the critical points between bosonic symmetry protected topological phases, *Nuclear Physics B* **919**, 470 (2017).
  - [51] S. Gozel, D. Poilblanc, I. Affleck, and F. Mila, Novel families of su(n) aklt states with arbitrary self-conjugate edge states, *Nuclear Physics B* **945**, 114663 (2019).
  - [52] T. Kennedy, Exact diagonalisations of open spin-1 chains, *Journal of Physics: Condensed Matter* **2**, 5737 (1990).
  - [53] L. Vanderstraeten, M. Mariën, F. Verstraete, and J. Haegeman, Excitations and the tangent space of projected entangled-pair states, *Physical Review B* **92**, 201111 (2015).
  - [54] L. Vanderstraeten, J. Haegeman, and F. Verstraete, Simulating excitation spectra with projected entangled-pair states, *Physical Review B* **99**, 165121 (2019).
  - [55] D. Poilblanc, N. Schuch, D. Pérez-García, and J. I. Cirac, Topological and entanglement properties of resonating valence bond wave functions, *Physical Review B* **86**, 014404 (2012).
  - [56] S. E. Nagler, D. A. Tennant, R. A. Cowley, T. G. Perring, and S. K. Satija, Spin dynamics in the quantum antiferromagnetic chain compound kcu<sub>3</sub>, *Physical Review B* **44**, 12361 (1991).
  - [57] D. A. Tennant, T. G. Perring, R. A. Cowley, and S. E. Nagler, Unbound spinons in the s=1/2 antiferromagnetic chain kcu<sub>3</sub>, *Physical Review Letters* **70**, 4003 (1993).
  - [58] M. Arai, M. Fujita, M. Motokawa, J. Akimitsu, and S. M. Bennington, Quantum spin excitations in the spin-peierls system cugeo<sub>3</sub>, *Physical Review Letters* **77**, 3649 (1996).
  - [59] M. Mourigal, M. Enderle, A. Klöpperpieper, J.-S. Caux, A. Stunault, and H. M. Rønnow, Fractional spinon excitations in the quantum heisenberg antiferromagnetic chain, *Nature Physics* **9**, 435 (2013).
  - [60] B. Lake, D. A. Tennant, J.-S. Caux, T. Barthel, U. Schollwöck, S. E. Nagler, and C. D. Frost, Multispinon continua at zero and finite temperature in a near-ideal heisenberg chain, *Physical Review Letters* **111**, 137205 (2013).
  - [61] B. Grenier, S. Petit, V. Simonet, E. Canévet, L.-P. Regnault, S. Raymond, B. Canals, C. Berthier, and P. Lejay, Longitudinal and transverse zeeman ladders in the ising-like chain antiferromagnet baco<sub>2</sub>v<sub>2</sub>o<sub>8</sub>, *Physical Review Letters* **114**, 017201 (2015).
  - [62] J. Haegeman, T. J. Osborne, and F. Verstraete, Post-matrix product state methods: To tangent space and beyond, *Physical Review B* **88**, 075133 (2013).
  - [63] S. B. Rutkevich, Energy spectrum of bound-spinons in the quantum ising spin-chain ferromagnet, *Journal of Statistical Physics* **131**, 917 (2008).

## APPENDIX: STRING ANSATZ FOR BROAD EXCITATIONS

In this appendix we provide the details of the extended quasiparticle ansatz for describing broad low-energy excitations (see Sec. IC in main text).

## 1. Implementation

We first recall that the quasiparticle ansatz is a momentum superposition of the uniform MPS ground state in which one tensor is distorted

$$|\Phi_p(B)\rangle = \sum_n e^{ipn} \left[ \begin{array}{c} \boxed{A} \quad \boxed{A} \quad \boxed{B} \quad \boxed{A} \quad \boxed{A} \\ s_{n-2} \quad s_{n-1} \quad s_n \quad s_{n+1} \quad s_{n+2} \end{array} \right]. \quad (1)$$

For further details on uniform MPS, and in particular of the gauge fixing, we refer to the tangent-space review in Ref. [18]. Here we just mention that we always work in the mixed gauge and that the distortion tensor  $B$  obeys the left gauge-fixing condition  $\sum_{s=1}^d A_L^{s\dagger} B^s = \sum_{s=1}^d B^{s\dagger} A_L^s = 0$  in which we assumed the ground-state tensor  $A$  to be in the left-canonical form  $\sum_s A_L^s A_L^s = 1$ .

The quasiparticle ansatz (1) describes local and low-energy excitations to extreme precision [24]. However, as the variational subspace on top of the MPS ground state is very localized, it is not expected to accurately capture the effect of large physical operators acting on the ground state [38]. Therefore, broad excitations such as the soliton bound states in the  $J_1 - J_2 - J_3$  model (see main text) are not well described by this ansatz.

In Ref. [38] it is suggested to increase the variational support by spreading the distortion over several sites

$$|\Phi_p(B)\rangle = \sum_n e^{ipn} \left[ \begin{array}{c} \boxed{A} \quad \boxed{A} \quad \boxed{B} \quad \boxed{A} \quad \boxed{A} \\ s_{n-2} \quad s_{n-1} \quad s_n \quad s_{n+1} \quad s_{n+2} \end{array} \right]. \quad (2)$$

The  $B$ -block in this ansatz contains  $D^2 d^N$  elements, where  $D$  is the bond dimension and  $d$  the physical dimension. By taking into account the gauge fixing  $D^2(d-1)d^{N-1}$  elements are truly variational. The exponential scaling in the number of distorted sites makes this ansatz hard to use, except for the paradigmatic AKLT-model [38, 62], for which the ground state can be exactly represented by an MPS with bond dimension 2.

A more efficient representation is given by a tensor decomposition of the  $B$ -block

$$|\Phi_p(B_1 \cdots B_N)\rangle = \sum_n e^{ipn} \left[ \begin{array}{c} \boxed{A} \quad \boxed{A} \quad \boxed{B_1} \quad \boxed{B_2} \quad \cdots \quad \boxed{B_N} \quad \boxed{A} \quad \boxed{A} \\ s_{n-2} \quad s_{n-1} \quad s_n \quad \dots \quad s_{n+N-1} \quad s_{n+N} \quad s_{n+N+1} \end{array} \right]. \quad (3)$$

Here the gauge fixing condition only applies on first tensor ( $B_1$ ), such that the other tensors in the decomposition ( $B_2, \dots, B_N$ ) are purely variational.

By this decomposition the number of variational parameters can be chosen to scale linear with  $N$ . This clearly depends on the choice of limiting bond dimension  $D_{\max}$  inside the excitation string. Now the excitation string can be seen as a finite-size subsystem on top of the ground state, and can be optimized by standard finite-size DMRG-methods [22] that are computationally efficient.

In order to construct such an efficient DMRG scheme to optimize over the excitation tensors  $B_1^{s_1} \dots B_N^{s_N+N-1}$  in (3), we need to construct the effective Hamiltonian for a one-site update

$$2\pi\delta(0)\mathbf{B}_i^\dagger H_{\text{eff}}^i(p)\mathbf{B}_i = \langle \Phi_p(B_1 \dots B_N) | \hat{H} | \Phi_p(B_1 \dots B_N) \rangle, \quad (4)$$

where the bold symbols denote the vectorized version of the corresponding tensor, and  $\hat{H} = \sum_n \hat{h}_{n, \dots, n+M-1}$  the many-body Hamiltonian that only consists of local  $M$ -body interactions. Two-site update schemes may be equally well considered, but this will make the construction of the effective Hamiltonians more cumbersome. The construction of  $H_{\text{eff}}^i(p)$  boils down to the knowledge of the matrix element at the right hand side of Eq. (4). Translation invariance implies that the terms in the matrix element contain maximally a double infinite sum over transfer matrices  $\sum_{s=1}^d A^s \otimes \bar{A}^s$ . But still we need to take into account all different relative positions of the local Hamiltonian  $\hat{h}$  with respect to all excitations tensors that appear in the bra and in the ket-layer. Here the left gauge fixing of the first excitation tensor significantly reduces the number of terms.

Once we have constructed  $H_{\text{eff}}^i(p)$ , we can update the  $i$ -th site by solving the generalized eigenvalue problem

$$H_{\text{eff}}^i(p)\mathbf{X}_i = \omega(p)N_{\text{eff}}^i(p)\mathbf{X}_i. \quad (5)$$

If the MPS ground state and the  $B$ -tensors are in the mixed canonical form at each update, the eigenvalue problem reduces to a standard problem, i.e.  $N_{\text{eff}}^i(p)$  is the unit matrix. By sweeping through the excitation string, the excitation energy is gradually lowered up to convergence. With the obvious initialization of  $B_2, \dots, B_N = A$ , the starting energy will be equal to the lowest energy obtained by (1). Higher energy excitations may be found by projecting away the lower-lying excitations.

## 2. Benchmarks

We demonstrate the accuracy of the string-ansatz by comparing its energy solution with the solution of the full problem given by Eq. (2) for the fundamental magnon at momentum  $p = \pi$  in the AKLT model. This comparison is shown in Tab. I. We raise the bond dimension inside the excitation string up to the limiting values  $D_{\text{lim}} = 54$  and  $D_{\text{lim}} = 108$ , this corresponds to an exact decomposition of the full  $B$ -tensor in terms of separate blocks up to respectively  $N = 7$  and  $N = 8$  sites. For  $N > \{7, 8\}$  the number of variational parameters scales linearly in the number of added sites, instead of exponentially in (2). For  $N > \{7, 8\}$  we can never recover the same precision as the original results in the first column, though the difference seems to be negligible in practice. However, because of the computational efficiency, we can go to a

$N$	tensor	string $D_{\text{lim}} = 54$	string $D_{\text{lim}} = 108$
1	.3703703703703	.370370370370370	.370370370370370
2	.3506345810861	.350634581086136	.350634581086135
3	.3501652022172	.350165202217295	.350165202217298
4	.3501291730768	.350129173076821	.350129173076823
5	.3501247689418	.350124768941853	.350124768941852
6	.3501242254394	.350124225439428	.350124225439427
7	.3501241645674	.350124164567495	.350124164567493
8	.3501241580969	.350124158096968	.350124158096949
9	.3501241574175	.350124157417571	.350124157417519
10	.3501241573460	.350124157346082	.350124157346044
11	.3501241573384	.350124157338518	.350124157338485
12	.3501241573376	.350124157337713	.350124157337683
13	-	.350124157337627	.350124157337597
14	-	.350124157337619	.350124157337586

TABLE I. Excitation energies of the magnon branch at momentum  $\pi$  of the AKLT model. The ansatz substitutes  $N$  sites in the MPS. The first column is copied from [38] (see table on pag. 34) and is obtained by the ansatz 2. The second and third column are obtained by the ansatz (3) in which the internal bond dimension of the string is limited to  $D_{\text{lim}} = 54$  and  $D_{\text{lim}} = 108$  respectively. The eigensolvers used to obtain these energies are reliable up to 14 digits (15 digits are shown in the second and third column, and 13 in the first).

higher number of sites. Consequently, we can recover and even slightly improve the precision obtained by optimizing Eq. (2).

We now consider the Ising model  $S = 1/2$  in a tilted magnetic field, the Hamiltonian is given by

$$\hat{H} = - \sum_i (\hat{\sigma}_i^x \hat{\sigma}_{i+1}^x + h_\perp \hat{\sigma}_i^z + h_\parallel \hat{\sigma}_i^x), \quad (6)$$

the parameter  $h_\perp$  describes a transverse field and the parameter  $h_\parallel$  an additional longitudinal field.

For  $h_\parallel = 0$  in the ordered regime far enough from the critical point, topological excitations as domain walls may occur. By applying the Jordan-Wigner transformation on the Hamiltonian, these domain walls can be represented as free fermions [63]. When a longitudinal field  $h_\parallel > 0$  is applied, the  $\mathbb{Z}_2$  symmetry is broken. This energetically favors one of the two previously degenerate ground states, and induces an attractive force between pairs domain walls – they form a state of bound spinons. When the applied field is not too large, the force can be modeled by the cost of adding one site that is in the ‘wrong’ ground state:  $\mu = 2h_\parallel \bar{m}$  where  $\bar{m} = (1 - h_\perp^2)^{1/8}$  [63]. Hence, the semi-classical Hamiltonian of the relative variables that describe the weakly confined spinons (or the slightly interacting fermions) just describes a particle that is moving in a linear potential. The time-independent Schrödinger equation for this Hamiltonian is the Airy equation. The low-lying energy spectrum is then approximated by the negative zero’s of the anti-symmetric Airy function [63]. At momentum

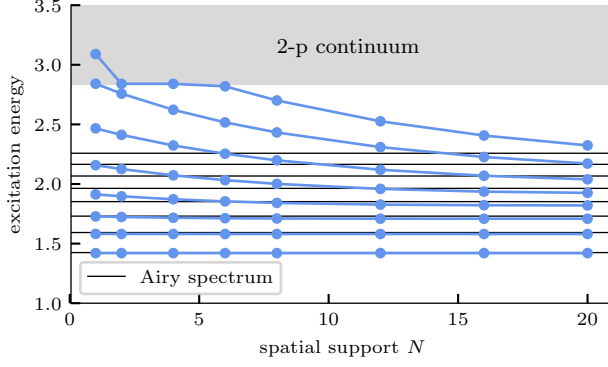


FIG. 11. Excitation energies at  $p = 0$  in the Ising model (6) for  $h_{\perp} = 0.7$  and  $h_{\parallel} = 0.0075$  as a function of the spatial support of the ansatz with  $D_{lim} = 40$ . By increasing  $N$  it becomes clear that the energies follow an Airy-like spectrum.

$p = 0$  the energy can be approximated as

$$E_n(0) \approx 4(1 - h_{\perp}) + \mu^{2/3} \left[ \frac{2h_{\perp}}{1 - h_{\perp}} \right]^{1/3} \xi_n. \quad (7)$$

with  $\xi_n$  determined by  $-\text{Ai}(-\xi_n) = 0$ . We applied the ansatz (1) and (3) at  $p = 0$  to calculate the excitations in this model for  $h_{\perp} = 0.7$  in the weak confining regime with  $h_{\parallel} = 0.0075$ . The results are shown in Fig. 11 together with the energies predicted by Eq. (7). The quasiparticle ansatz ( $N = 1$ ) does not yet reveal the full Airy behavior of the spectrum. By increasing the spatial support of the excitation ansatz, we however observe a fast decrease of the excitation energies. The higher the excitation energy, the more significant the decrease of the energy. The highest excitation under study remains stuck in the continuum for the smallest  $N$ . The observation that the energies are always lower than the ones predicted from (7), has probably to do with the effect of higher order terms in the expansion of the kinetic energy of the spinons. By going to a strong longitudinal field, we expect faster convergence as a function of  $N$  but however stronger deviations from the Airy spectrum.